



Journal Name

ARTICLE

# Water-soluble luminescent hybrid aminoclay grafted with lanthanide complexes synthesized by Michael-like addition reaction and its gas sensing application in PVP nanofiber

Received 00th January 20xx,

Qing-Feng Li,<sup>a</sup> Lin Jin,<sup>a</sup> Lili Li,<sup>a</sup> Wenpei Ma,<sup>a</sup> Zhenling Wang,<sup>\*a</sup> and Jianhua Hao<sup>\*b</sup>

Accepted 00th January 20xx

DOI: 10.1039/x0xx00000x

www.rsc.org/

Aminoclay has been used as a scaffold for lanthanide complexes and dye molecules for light harvesting application. However, these syntheses are mainly based on non-covalent electrostatic attraction between aminoclay and guest moleculars. Herein we develop a strategy to synthesize luminescent aminoclay by Michael-like addition reaction between amino-group of aminoclay and Michael acceptor group. UV absorbance, photoluminescence and phosphorescence spectra studies confirmed that luminescent lanthanide complexes were covalently grafted onto the aminoclay. We found that the hybrid aminoclays (AC-Ln(DPA)<sub>n</sub>) exhibit favorable luminescent properties coupled with good water-solubility. Furthermore, the luminescent aminoclay can be incorporated into water-soluble polyvinylpyrrolidone (PVP) to obtain highly luminescent, physically crosslinked nanofiber by electrospinning technology. Interestingly, an exposure of the nanofiber to HCl vapors can cause a significant quenching of Eu<sup>3+</sup> luminescence, while a remarkable luminescence enhancement occurred upon exposure of the acid-treated nanofiber to Et<sub>3</sub>N vapors. Further studies indicated that this reversible luminescence change is due to the dissociation and recovery of Eu<sup>3+</sup> complexes by HCl and Et<sub>3</sub>N vapors. The results present a promising gas sensing application based on the developed hybrid luminescent materials.

## Introduction

Layered clay materials that can be synthesized to tune their surface-charge properties have recently emerged as promising scaffold for construction of functional materials.<sup>1-3</sup> However, many practical applications of clay have been limited due to their low water-dispersity. In comparison, a new class of synthetic amino-functionalized magnesium silicate clay named as aminoclay (AC) shows high water-solubility because it can be self-exfoliated in water by the electrostatic repulsive forces between protonated amino-groups,<sup>4</sup> and this inherent property makes it useful as metal catalyst or drug delivery carriers, guest molecular scaffold, etc.<sup>5-8</sup> It should be mentioned that great efforts have been made toward modifying AC with some luminophores to expand its optical applications in recent years.<sup>9-13</sup> For instance, George et al. developed a novel class of white light-emitting soft-material by noncovalent co-assembly of AC and ionic chromophores.<sup>10</sup> Li and co-workers synthesized multi-color luminescent hybrid materials based on AC and lanthanide complexes, and the as-prepared hybrid material shows temperature-dependent luminescent property.<sup>12</sup>

Wang et al. prepared flexible luminescent polyvinylalcohol/AC composite films doped with lanthanide complexes.<sup>13</sup> However, these synthetic approaches are mainly based on the noncovalent ion-pairs interaction between AC and guest moleculars. In view of the fact that AC are able to be completely protonated in neutral solution to form amino-positive ion, only the negatively charged molecules can be incorporated into AC *via* ion exchange.

Michael-like addition reaction has been rarely applied in preparation of hybrid luminescent materials, although it has been a widely used chemical modification technology that is well established in materials chemistry<sup>14,15</sup> and protein science.<sup>16,17</sup> It is well known that amino-group, a strong nucleophilic group, can react with Michael acceptors *via* forming a N-C bond, which is stable in the presence of acid or alkali solution.<sup>18</sup> Recently, we have synthesized a bifunctional chelating agent named as 4-vinylpyridine-2, 6-dicarboxylic acid, which contains: (1) a Michael acceptor moiety that can react with nucleophilic group *via* Michael-like addition reaction,<sup>19</sup> and (2) a pyridine-2, 6-dicarboxylic acid (DPA) moiety that can sensitize the luminescence of Tb<sup>3+</sup> or Eu<sup>3+</sup> ions.<sup>20</sup> Thus, this will provide a new approach for covalent modification of aminoclay by means of Michael-like addition reaction.

In this work, we prepared a novel hybrid luminescent material by covalent attachment of 4-vinylpyridine-2, 6-dicarboxylic acid to AC. In this strategy, the amino-group in AC acts as Michael donor which can react with 4-vinylpyridine-2, 6-dicarboxylic acid by Michael-like addition reaction. The obtained hybrid materials exhibit excellent water-solubility and their aqueous solution show

<sup>a</sup> The Key Laboratory of Rare Earth Functional Materials and Applications, Zhoukou Normal University, Zhoukou 466001, Henan, P. R. China.

E-mail: liqingf335@163.com, zlwang2007@hotmail.com; Fax/Tel: +86-394-8178518

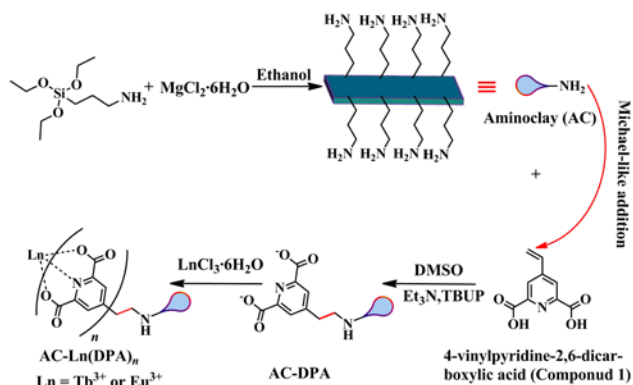
<sup>b</sup> Department of Applied Physics, The Hong Kong Polytechnic University, Hong Kong, P. R. China. E-mail: jh.hao@polyu.edu.hk

\*Electronic Supplementary Information (ESI) available: XRD, CIE, phosphorescence spectra, FT-IR spectra and luminescence decay curves. See DOI: 10.1039/x0xx00000x

bright visible emission under UV irradiation. This approach is expected to provide a useful and universally applicable strategy for preparation of hybrid materials. Through this strategy, lanthanide complexes could be grafted onto the functional matrix containing a nucleophilic group such as amino or thiol group. Meanwhile, transition metal complexes could also be grafted onto the functional matrixes by designing suitable heteroleptic ligand. In addition, the incorporation of layered clay into polymers can usually adjust their performance and application.<sup>21, 22</sup> Therefore, the luminescent composite nanofibers from modified AC and polyvinylpyrrolidone (PVP) were prepared *via* the electrospinning process, in which AC moiety acts as a crosslinker for PVP<sup>23</sup>, and the resulting nanofiber exhibits good acid-base gas sensitive properties.

## Results and discussion

The proposed synthesis procedure of hybrid luminescent aminoclay was illustrated in Scheme 1. Firstly, 4-vinylpyridine-2, 6-dicarboxylic acid (compound 1)<sup>20</sup> and aminoclay<sup>12,24</sup> were synthesized as previously described, respectively. Then, the hybrid aminoclay (AC-DPA) was prepared through the Michael-like addition reaction of aminoclay and compound 1 in dimethylsulfoxide (DMSO) solution, and it is worth noting that the addition reaction does not proceed well in the absence of triethylamine (Et<sub>3</sub>N) and tributylphosphine (TBUP). Finally, the hybrid luminescent aminoclays (AC-Ln(DPA)<sub>n</sub>, Ln = Tb or Eu) were obtained by assembling with AC-DPA and lanthanide ion in ethanol.



**Scheme 1** Proposed synthesis procedure of the hybrid luminescent aminoclay AC-Ln(DPA)<sub>n</sub>.

The UV absorbance spectra of pyridine-2, 6-dicarboxylic acid (DPA), compound 1, AC-DPA, AC-Ln(DPA)<sub>n</sub> are presented in Fig. 1. It can be seen that the compound 1 exhibits two obvious absorption peaks at 290 and 300 nm, assigned to  $\pi \rightarrow \pi^*$  electronic transition of the conjugated group (Fig. 1b). However, the UV spectra of AC-DPA, AC-Tb(DPA)<sub>n</sub>, AC-Eu(DPA)<sub>n</sub> (Fig. 1c to e) showed a clear blue-shift compared with that of compound 1, which is ascribed to the addition reaction of compound 1 and aminoclay.<sup>25</sup> Furthermore, the UV spectra of AC-DPA, AC-Tb(DPA)<sub>n</sub> and AC-Eu(DPA)<sub>n</sub> are very similar to those of DPA (Fig. 1a), which also proved that the electron deficient double bond of compound 1 was successfully reacted with

amino-group of aminoclay in this addition reaction. However, there was little change in the UV absorbance spectrum of the mixture of compound 1 and AC in the absence of Et<sub>3</sub>N and TBUP within 7 days. This result showed that the addition of Et<sub>3</sub>N and TBUP greatly accelerated the rate of the addition reaction.

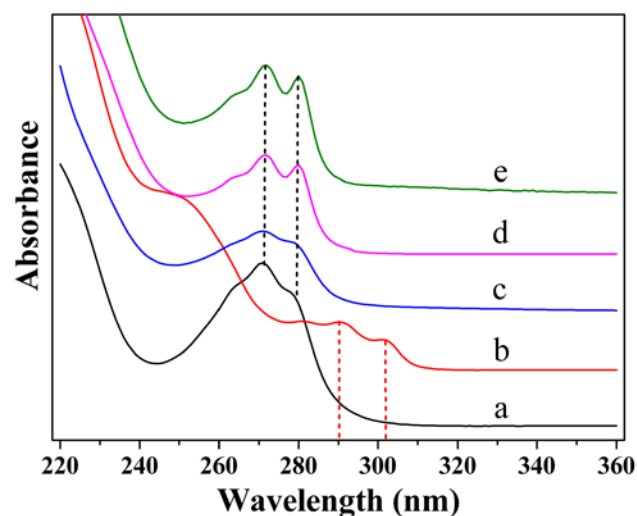


**Fig. 1** UV absorbance spectra of DPA (a), compound 1 (b), AC-DPA (c), AC-Tb(DPA)<sub>n</sub> (d) and AC-Eu(DPA)<sub>n</sub> (e) in aqueous solution (pH 7.4).

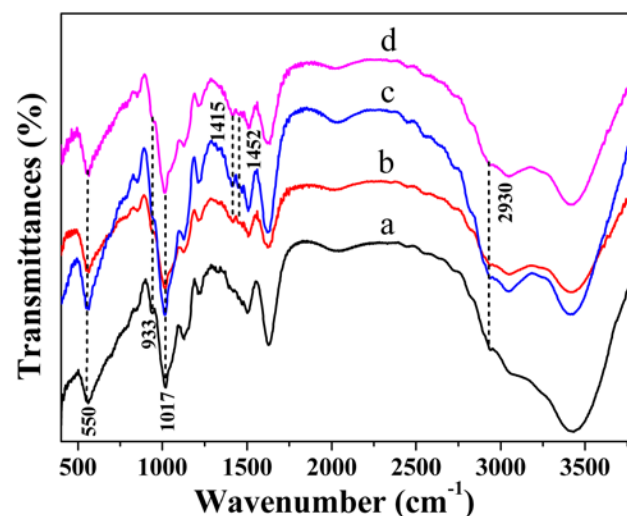


**Fig. 2** FT-IR spectra of AC (a), AC-DPA (b), AC-Tb(DPA)<sub>n</sub> (c) and AC-Eu(DPA)<sub>n</sub> (d).

The FT-IR spectra of aminoclay and functionalized aminoclay were displayed in Fig. 2. The absorption bands located at 1017 cm<sup>-1</sup> can be ascribed to asymmetric stretching vibration of Si-O, and the bands centered around 550 and 933 cm<sup>-1</sup> are associated with the stretching vibrations of the Mg-O groups and deformation vibration of inner Mg-OH groups,<sup>26,27</sup> respectively (Fig. 2a to d). Meanwhile, the peak at 2930 cm<sup>-1</sup> ( $\nu_{as}$ , C-H), originating from the -CH<sub>2</sub>CH<sub>2</sub>CH<sub>2</sub>NH<sub>2</sub> groups, is a further evidence to support the successful synthesis of aminoclay. After reacting with compound 1, two new bands corresponding to the skeleton vibration of pyridine ring (C=C or C=N) appeared at 1415 and 1452 cm<sup>-1</sup> (Fig. 2b to d),

which demonstrates the successful grafting of DPA group onto the aminoclay. <sup>20</sup> Moreover, XRD results showed that AC-Tb(DPA)<sub>n</sub>, AC-Eu(DPA)<sub>n</sub> and AC have a similar talc-like structure (Fig. S1). <sup>6</sup>

The optical properties of AC-Tb(DPA)<sub>n</sub> and AC-Eu(DPA)<sub>n</sub> were investigated by photoluminescence (PL) spectra. Both of the excitation spectra show a broad excitation band with a maximum at 280 nm, which can be attributed to the absorption of the lanthanide complexes, including ligand and lanthanide ions (Fig. 3a and c). This result shows that these two kinds of hybrid luminescence aminoclays can be excited by the ultraviolet (UV) light with identical wavelength, but emit different luminous color. As expected, under UV light excitation (280 nm), AC-Tb(DPA)<sub>n</sub> exhibits the characteristic emission peaks at 491 542, 582 and 621 nm, attributed to <sup>5</sup>D<sub>4</sub>→<sup>7</sup>F<sub>J</sub> (J = 6, 5, 4, 3) transitions of Tb<sup>3+</sup> ion, respectively. Among these emissions the emission corresponding to <sup>5</sup>D<sub>4</sub>→<sup>7</sup>F<sub>5</sub> is the strongest one (Fig. 3b). <sup>28-31</sup> While, under identical excitation, AC-Eu(DPA)<sub>n</sub> gives the characteristic emission peaks of Eu<sup>3+</sup> at 594, 615, 649 and 695 nm, assigned to the <sup>5</sup>D<sub>0</sub>→<sup>7</sup>F<sub>J</sub> (J = 0, 1, 2, 3, 4) transitions of Eu<sup>3+</sup> ion with the <sup>5</sup>D<sub>0</sub>→<sup>7</sup>F<sub>2</sub> transition as the most prominent one (Fig. 3d). <sup>32-36</sup> No broad emission band of the organic ligand can be observed in the emission spectra, implies that the energy transfer occurs from the ligand to the central Ln<sup>3+</sup> ion (Ln = Tb or Eu). As observed by luminescent photos, AC-Tb(DPA)<sub>n</sub> and AC-Eu(DPA)<sub>n</sub> show bright green and red emissions under UV light excitation (insets of Fig. 3b and d). The CIE (Commission Internationale de l'Eclairage) chromaticity coordinates also indicate that the emission of AC-Tb(DPA)<sub>n</sub> and AC-Eu(DPA)<sub>n</sub> lie in green (x = 0.33, y = 0.57) and red (x = 0.66, y = 0.34) region, respectively (Fig. S2).

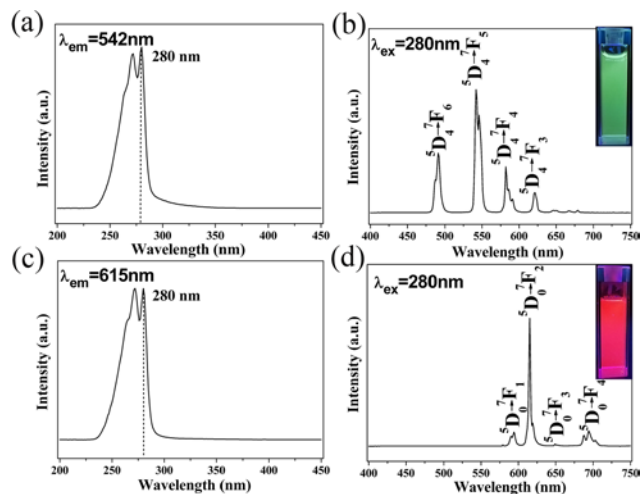


**Fig. 3** PL excitation and emission spectra of AC-Tb(DPA)<sub>n</sub> (a, b) and AC-Eu(DPA)<sub>n</sub> (c, d) in aqueous solution, and the insets of Fig. 3b and d are digital photos of AC-Tb(DPA)<sub>n</sub> (green) and AC-Eu(DPA)<sub>n</sub> (red) solution excited by UV light (254 nm).

The lifetime values of the excited state <sup>5</sup>D<sub>4</sub> (Tb<sup>3+</sup>) in AC-Tb(DPA)<sub>n</sub> and <sup>5</sup>D<sub>0</sub> (Eu<sup>3+</sup>) in AC-Eu(DPA)<sub>n</sub> can be determined by the luminescent decay curves (Fig. 4). Both the decay curves could be well fitted by a double-exponential function described as  $I = A_1 \exp(-t/\tau_1) + A_2 \exp(-t/\tau_2)$ , where  $\tau_1$  and  $\tau_2$  stand for the slow and fast terms of the luminescent lifetime respectively, and  $A_1$  and  $A_2$  are the

corresponding pre-exponential factors. These results imply the presence of different luminescent unit in these hybrid materials. As described in the literature, there are three types of complexes formed by dipicolinic acid (DPA) and Ln<sup>3+</sup>: [Ln(DPA)]<sup>+</sup>, [Ln(DPA)<sub>2</sub>]<sup>0</sup>, [Ln(DPA)<sub>3</sub>]<sup>3-</sup>. Based on the results, we speculate that there are two main forms of complexes present in these materials, the average coordination environment of Tb<sup>3+</sup> or Eu<sup>3+</sup> is not uniform. Therefore, the decay curves were fitted by a double-exponential function. We use  $n$  to represent the real mole ratio of ligand to metal ion in AC-Ln(DPA)<sub>n</sub>. The average lifetime can be calculated using the following equation.

$$\tau = (A_1\tau_1^2 + A_2\tau_2^2) / (A_1\tau_1 + A_2\tau_2)$$

According to the fitting results, the lifetime values of AC-Tb(DPA)<sub>n</sub> and AC-Eu(DPA)<sub>n</sub> are determined to be 1.64 and 1.50 ms, respectively.

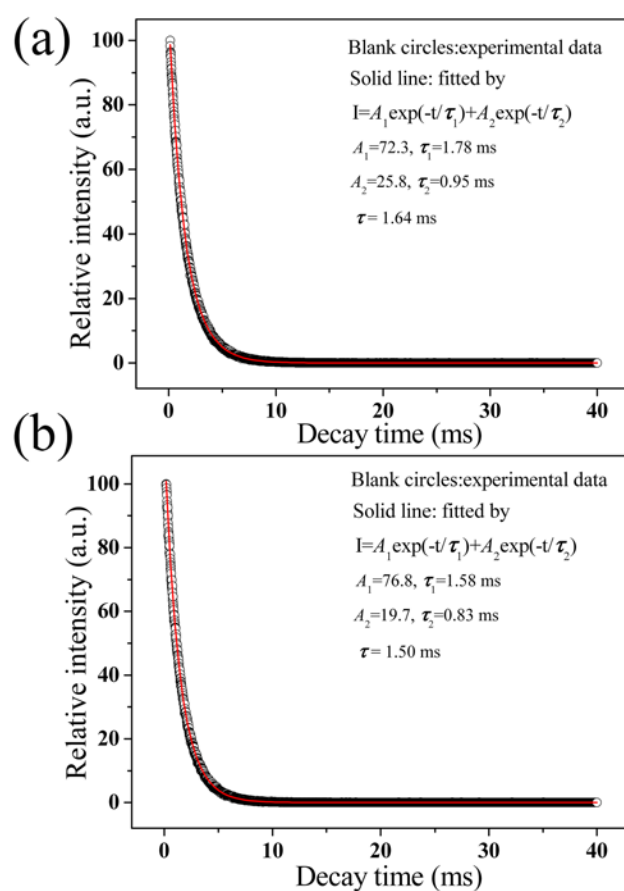


**Fig. 4** Luminescence decay curves of AC-Tb(DPA)<sub>n</sub> (a) and AC-Eu(DPA)<sub>n</sub> (b).

As reported by other researchers, pyridine-2, 6-dicarboxylic acid (DPA) is an efficient tridentate ligand for sensitizing the luminescence of Tb<sup>3+</sup> or Eu<sup>3+</sup>. <sup>37-39</sup> Na<sub>3</sub>[Tb(DPA)<sub>3</sub>] exhibits bright green emission upon an excitation of UV light with a wavelength of 280 nm. <sup>38</sup> However, when compound 1 and Tb<sup>3+</sup> ion were mixed together with a molar ratio of 3:1 under neutral pH condition, no characteristic green emission of Tb<sup>3+</sup> ion was observed for the above mixture by excitation of the same UV light. <sup>20</sup> Generally,

intramolecular energy transfer from the triplet state of the organic ligand to the resonance level of  $\text{Ln}^{3+}$  ion is regarded as a critical factor affecting the luminescence of lanthanide complexes. The triplet state energy level of compound 1 determined by the corresponding phosphorescence spectrum of  $\text{Na}_3[\text{Gd}(\text{1})_3]$  at 77 K was  $20833 \text{ cm}^{-1}$  (Fig. S3), which is very close to  $^5\text{D}_4$  for  $\text{Tb}^{3+}$  ( $20430 \text{ cm}^{-1}$ ). However, previous studies showed that a close match between the resonance level of  $\text{Tb}^{3+}$  ion and the triplet state of the organic ligand is not desirable, because energy back-transfer from the excited  $\text{Tb}^{3+}$  ion to the organic ligand will occur,<sup>40,41</sup> leading to  $\text{Tb}^{3+}$  luminescence quenching (Fig. 5). As for  $\text{AC-Tb}(\text{DPA})_n$ , the amino-group of aminoclay was reacted with electron-deficient C=C of compound 1 to generate a DPA residue (Scheme 1), and the triplet energy level of DPA ( $26600 \text{ cm}^{-1}$ ) is higher than the emitting level of  $\text{Tb}^{3+}$  ( $^5\text{D}_4$ ,  $20430 \text{ cm}^{-1}$ ). Therefore, the DPA residue can act as an antenna ligand for sensitizing the luminescence of  $\text{Tb}^{3+}$  ion (Fig. 5). In order to determine if the DPA residue can be generated only through the Michael-like reaction of amino-group and compound 1, we simply mixed compound 1,  $\text{Et}_3\text{N}$  and TBUP in DMSO for two days, and then  $\text{Tb}^{3+}$  ions was added to the above solution, no characteristic emission of  $\text{Tb}^{3+}$  ions was observed under the irradiation of UV light, which shows that no DPA residue was generated in the absence of amino group. This result indirectly suggests that the DPA residue was really grafted onto aminoclay via Michael-like addition reaction.

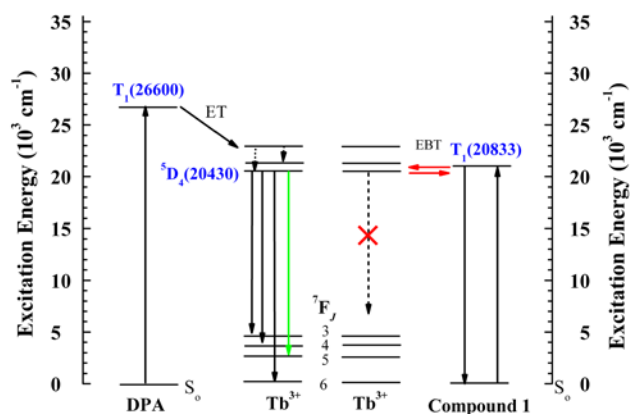


**Fig. 5** Simplified energy diagram of DPA, compound 1 and  $\text{Tb}^{3+}$ ; ET: Energy transfer, EBT: Energy back-transfer.

It is well known that polyvinylpyrrolidone (PVP) is a water-soluble, biocompatible and nontoxic organic polymer. This material has excellent thermal stability, adsorption, adhesion and film-forming ability, which makes it an ideal scaffold for design of various functional materials with different states such as film, hydrogel and nanofiber.<sup>42-44</sup> Moreover, the incorporation of clay into PVP matrix usually improves the physicochemical properties of the resulting composites. Hence, it is reasonable to envisage the combination of PVP and the functionalized aminoclay to afford a novel luminescent material. By means of electrospinning technique, we prepared a kind of luminescent composite nanofibers using PVP and  $\text{AC-Ln}(\text{DPA})_n$  as precursors, and the morphology of the nanofibers were investigated by scanning electron microscopy (SEM). As shown in Fig. 6, both of the composite nanofibers with diameter of  $460 \pm 110 \text{ nm}$  have a relatively uniform and smooth surface, indicating

that  $\text{AC-Ln}(\text{DPA})_n$  were well embedded in the PVP matrix. FT-IR analysis was further carried out to verify the interactions between the luminescent aminoclay and PVP. As shown in Fig. S4a, the peak at  $1657 \text{ cm}^{-1}$  could be ascribed to the stretching vibration of C=O of PVP.<sup>23</sup> However, this band was blue-shifted after modification by luminescent aminoclay (Fig. S4b and c), suggesting the presence of hydrogen bonding between the  $\text{AC-Ln}(\text{DPA})_n$  and PVP.

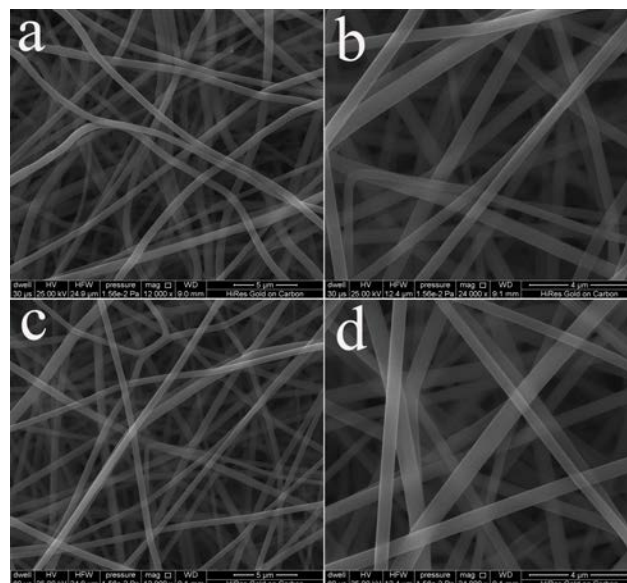


**Fig. 6** SEM image of PVP-AC- $\text{Tb}(\text{DPA})_n$  (a, b) and PVP-AC- $\text{Eu}(\text{DPA})_n$  (c, d).

The successful formation of PVP-AC- $\text{Ln}(\text{DPA})_n$  was also confirmed by optical studies. As shown in inset of Fig. 7b and d, under irradiation of 254 nm UV lamp, PVP-AC- $\text{Tb}(\text{DPA})_n$  and PVP-AC- $\text{Eu}(\text{DPA})_n$  emitted bright green and red light respectively. And the characteristic emission peaks of  $\text{Tb}^{3+}$  at 491, 542, 582 and 621 nm and  $\text{Eu}^{3+}$  ion at 594, 615, 649 and 695 nm were also observed in the corresponding PL spectra (Fig. 7b and d). The optical data like excitation wavelength ( $\lambda_{\text{ex}}$ ), emission wavelength ( $\lambda_{\text{em}}$ ), lifetimes ( $\tau$ ), CIE coordinates and quantum efficiency ( $\eta$ ) of  $\text{AC-Ln}(\text{DPA})_n$  and PVP-AC- $\text{Ln}(\text{DPA})_n$  are listed in Table S1. It appears that the quantum efficiency of PVP-AC- $\text{Ln}(\text{DPA})_n$  was higher than that of the corresponding  $\text{AC-Ln}(\text{DPA})_n$ , and the other optical data of PVP-AC- $\text{Ln}(\text{DPA})_n$  are very similar to that of  $\text{AC-Ln}(\text{DPA})_n$  (Table 1, Fig. S5 and Fig. S6). There may be two factors leading to the higher luminescence efficiency of PVP-AC- $\text{Ln}(\text{DPA})_n$ : 1) the interaction between PVP and  $\text{Ln}^{3+}$ ,<sup>45</sup> including coordination<sup>46</sup>; and 2) embedding of PVP. Therefore, the non-radiative transition of  $\text{Ln}^{3+}$  will decrease due to these two factors, and the quantum efficiency of PVP-AC- $\text{Ln}(\text{DPA})_n$  is higher than that of the corresponding  $\text{AC-Ln}(\text{DPA})_n$ .

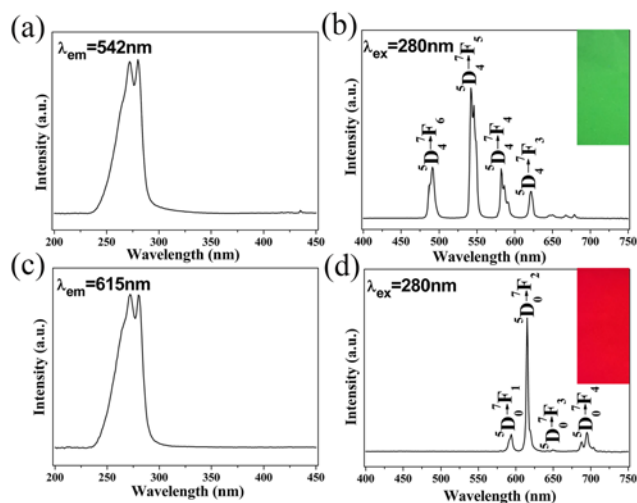


**Fig. 7** PL excitation and emission spectra of PVP-AC-Tb(DPA)<sub>n</sub> (a, b) and PVP-AC-Eu(DPA)<sub>n</sub> (c, d), and inset of Fig. 7b and d are the digital photos of PVP-AC-Tb(DPA)<sub>n</sub> and PVP-AC-Eu(DPA)<sub>n</sub> excited by UV light (254 nm).

As mentioned above, PVP-AC-Ln(DPA)<sub>n</sub> have prominent luminescent properties and proton-binding capacity, these characteristics make them promising candidate materials for acid gas sensor.<sup>47, 48</sup> As expected, after exposure of PVP-AC-Eu(DPA)<sub>n</sub> to HCl vapors, the luminescence intensity was concomitantly decreased by gradual increasing concentration of HCl vapor from 0 to 200 ppm, and then decreased slightly with further increasing of the HCl concentration (Fig. 8a). Fig. 8b shows a plot of  $I_0/I$  versus the HCl vapors concentration ([HCl]), which exhibits a good linear correlation at low HCl concentration, and the linear equation can be described by the Stern-Volmer equation:  $I_0/I = K_{sv}[HCl] + 1$ .<sup>49, 50</sup> Where  $I_0$  and  $I$  are the luminescence intensity of PVP-AC-Eu(DPA)<sub>n</sub> in the absence and presence of HCl vapors, respectively,  $K_{sv}$  is the quenching constant (ppm<sup>-1</sup>). The quenching constant ( $K_{sv}$ ) was calculated as 0.05 ppm<sup>-1</sup>, and the detection limit was determined to be 0.2 ppm for HCl vapors. Moreover, the time-dependent emission spectra after exposure of PVP-AC-Eu(DPA)<sub>n</sub> to HCl vapor were investigated. As shown in Fig. 8c and d, the emission intensity of PVP-AC-Eu(DPA)<sub>n</sub> decreased continuously upon exposure to the HCl vapor over the time range of 0-10 s, and a 75 % quenching of the emission intensity at 615 nm was found within 2 s, which indicated that PVP-AC-Eu(DPA)<sub>n</sub> is very sensitive to HCl gas. Meanwhile, we found that other volatile strong acids such as nitric acid and trifluoroacetic acid exhibit significant luminescence quenching effect for PVP-AC-Eu(DPA)<sub>n</sub>, however, nonvolatile or weak organic acids (sulfuric acid, phosphoric acid, phosphorous acid, propionic acid, acetic acid) show a slight effect on the luminescence intensities of PVP-AC-Eu(DPA)<sub>n</sub>, and a moderate quenching effect was found in presence of formic acid (Fig. S7).

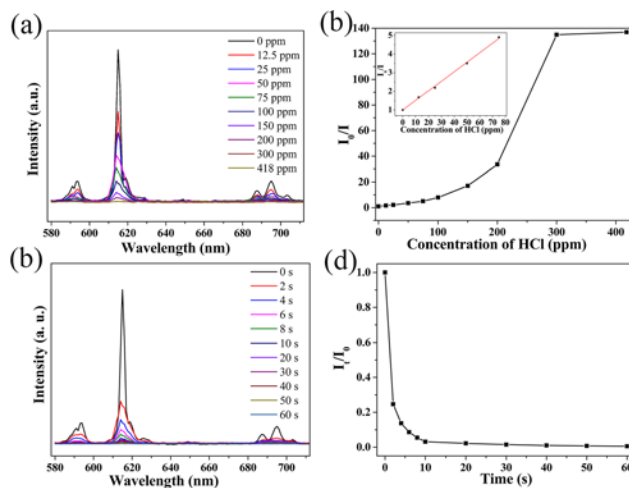


**Fig. 8** Concentration-dependent luminescence spectra of PVP-AC-Eu(DPA)<sub>n</sub> after exposure to different concentrations of HCl vapors (a), inset is Plot of Stern-Volmer plot for the response to HCl vapors (b), time-dependent luminescence spectra after exposure of PVP-AC-Eu(DPA)<sub>n</sub> to HCl vapors (c),

Interestingly, the addition of this acid vapors treated sample to Et<sub>3</sub>N vapors for 60 s causes a significant recovery of the luminescence intensity at 615 nm (Fig. 9). Meanwhile, the broad excitation band ranging from 230 to 300 nm re-emerged in the corresponding excitation spectrum (Fig. S8, red line). This reversible luminescence change can also be observed by naked eye under a UV-lamp (insets of Fig. 9). It is plausible that the gas sensitive property of PVP-AC-Eu(DPA)<sub>n</sub> is mainly due to the dissociation of the Eu<sup>3+</sup> complex in acidic medium. The high proton strength makes it easier for the carboxyl group to bind protons than Eu<sup>3+</sup> ion, which leads to the quenching of the luminescence. In contrast, the deprotonated carboxyl ligand can coordinate with Eu<sup>3+</sup> ion to form a stable luminescent complex in Et<sub>3</sub>N vapors (Fig. S9). Our analysis can be further confirmed by IR spectrum. As shown in Fig. S10, upon treatment with HCl vapor, a new band at 1747 cm<sup>-1</sup> corresponding to the C=O stretching vibration in -COOH appears in the IR spectrum (Fig. S10a),<sup>39</sup> indicating that the Eu<sup>3+</sup> complex was dissociated into free ligand and Eu<sup>3+</sup> ion by HCl vapors. However, this band is not observable after the nanofiber was further treatment with Et<sub>3</sub>N vapors. Moreover, two new bands at 2495, 2601 cm<sup>-1</sup> corresponding to the N-H stretching vibration of Et<sub>3</sub>N hydrochloride (Fig. S10c) are present (Fig. S10b), proving that the acidic sites on the HCl vapors treated sample was neutralized by Et<sub>3</sub>N vapors. Moreover, the acid/base controlled emission on-off switching characteristic of PVP-AC-Eu(DPA)<sub>n</sub> were investigated by monitoring the emission intensity changes at 615 nm upon exposure to HCl and Et<sub>3</sub>N vapors. It is found that PVP-AC-Eu(DPA)<sub>n</sub> displays good reversibility after exposure to 5 cycles of HCl vapors alternated with Et<sub>3</sub>N vapors (Fig. S11).

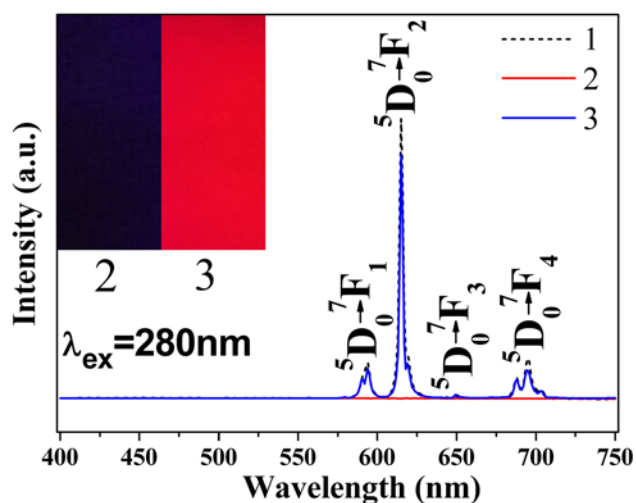


**Fig. 9** Emission spectra of PVP-AC-Eu(DPA)<sub>n</sub>, before (1) and after exposure to HCl vapors (2) and then Et<sub>3</sub>N vapors (3), and inset of Fig. 9 are digital photos of PVP-AC-Eu(DPA)<sub>n</sub> excited by UV light (254 nm) after exposure to HCl vapors (2) and then Et<sub>3</sub>N vapors (3).

## Conclusions

In summary, we demonstrate an effective strategy based on Michael-like addition reaction to synthesize the luminescent aminoclay. Optical analysis revealed that lanthanide complexes were successfully covalently grafted onto the AC by this strategy. The catalysts (Et<sub>3</sub>N and TBUP) play a key role in this addition reaction of AC and compound 1. Moreover, the as-prepared AC-Ln(DPA)<sub>n</sub> can be used as the crosslinker for fabricating luminescent PVP nanofiber, which can sense to both HCl and Et<sub>3</sub>N vapors. The results indicate that the protonation and deprotonation of carboxylic acid ligand are responsible for the reversible luminescence switching. Thus, we expect that our strategy will stimulate new opportunities in the design of multifunctional hybrid AC for exploitation in luminescent gas sensing.<sup>51,52</sup>

## Experimental section

4-vinylpyridine-2, 6-dicarboxylic acid (compound 1)<sup>20</sup> and aminoclay<sup>12,24</sup> were synthesized as previously reported.

### Synthesis of hybrid aminoclay (AC-DPA)

Aminoclay (0.5 g), 4-vinylpyridine-2, 6-dicarboxylic acid (20 mg), tributylphosphine (0.1 mL) and triethylamine (1.0 mL) were added to 8 mL of dimethyl sulphoxide (DMSO). The resulting mixture was stirred at room temperature for about 24 h. The suspension was centrifuged and the solid residue was washed with absolute ethanol, and then dried under vacuum at 50 °C for 8 h.

### Synthesis of hybrid luminescent aminoclay (AC-Ln(DPA)<sub>n</sub>)

AC-DPA (0.2 g) was dispersed in absolute ethanol (5 mL), and then LnCl<sub>3</sub>·6H<sub>2</sub>O (10 mg, Ln: Tb or Eu) was added to the above mixture. After stirred at room temperature for about 12 h, the mixture was centrifuged and the obtained solid was washed thoroughly with absolute ethanol.

### Synthesis of hybrid luminescent PVP nanofibers (PVP-AC-Ln(DPA)<sub>n</sub>)

AC-Ln(DPA)<sub>n</sub> (40 mg) was dissolved to deionized water (0.25 mL), the pH was adjusted to 7-8 with 2 mol/L hydrochloric acid. And then ethanol (1 mL), polyvinylpyrrolidone (PVP, Mw: 1.3×10<sup>6</sup>, 0.2 g) was added to the above solution. After stirred at room temperature for about 24 h, the nanofibers were prepared by electrospinning technology.

### Exposure to HCl/Et<sub>3</sub>N vapors

30 mg PVP-AC-Eu(DPA)<sub>n</sub> was put in a 25 mL glass beaker, and different concentration dry HCl gas was added to a 250 mL sealed container, and then the glass beaker placed into the sealed container for 60s. The same procedure was used in Et<sub>3</sub>N sensing, except that 3 mL dry Et<sub>3</sub>N was used in place of HCl gas.

## Characterization

Ultraviolet (UV) absorption spectrum was performed with a Lambda 35 (PerkinElmer) UV-vis spectrophotometer. FT-IR spectrum was recorded with a Thermo Nicolet 5700 spectrophotometer within the wavenumber range 4000-400 cm<sup>-1</sup> (KBr pellet). Powder X-ray diffraction (XRD) data were obtained on a Bruker D8 advance X-ray diffractometer. Scanning electron microscopy (SEM) images were obtained with a FEI Quanta 200 electron microscope. The luminescence spectra and lifetimes were determined using an Edinburgh FLS920P spectrofluorimeter. Quantum efficiency was measured by an integrating sphere whose inner face was coated with Benflect.

## Acknowledgements

This work is financially supported by the National Natural Science Foundation of China (no. 21401218, 51572303, 21477167), the Innovation Scientists and Technicians Troop Construction Projects of Henan Province (2013259), the Program for Innovative Research Team (in Science and Technology) in University of Henan Province (no.14IRTSTHN009). Key scientific and technological project of Henan Province (172102410024). High Level Personnel Fund of Zhoukou Normal University (ZKNU2013006).

## Notes and references

- 1 A. J. Patil and S. Mann, *J. Mater. Chem.*, 2008, **18**, 4605-4615.
- 2 L. Z. Zhao, C. H. Zhou, J. Wang, D. S. Tong, W. H. Yu and H. Wang, *Soft Matter*, 2015, **11**, 9229-9246.
- 3 S. J. Choi, J. M. Oh and J. H. Choy, *J. Mater. Chem.*, 2008, **18**, 615-620.
- 4 N. T. Whilton, S. L. Burkett and S. Mann, *J. Mater. Chem.*, 1998, **8**, 1927-1932.
- 5 K. K. R. Datta, M. Eswaramoorthy and C. N. R. Rao, *J. Mater. Chem.*, 2007, **17**, 613-615.
- 6 K. K. R. Datta, A. Achari and M. Eswaramoorthy, *J. Mater. Chem. A*, 2013, **1**, 6707-6718.

- 7 S. H. Wang, H. Cao, Y. M. Zhong, Y. H. Yang and Z. Z. Shao, *J. Mater. Chem. B*, 2016, **4**, 4295-4301.
- 8 A. Jain, A. Achari, N. Mothi, M. Eswaramoorthy and S. J. George, *Chem. Sci.*, 2015, **6**, 6334-6340.
- 9 K. V. Rao, K. K. R. Datta, M. Eswaramoorthy and S. J. George, *Angew. Chem. Int. Ed.*, 2011, **50**, 1179-1184.
- 10 K. V. Rao, K. K. R. Ratta, M. Eswaramoorthy and S. J. George, *Adv. Mater.*, 2013, **25**, 1713-1718.
- 11 T. R. Wang, X. Y. Yu, Z. Q. Li, J. Wang and H. R. Li, *RSC Adv.*, 2015, **5**, 11570-11576.
- 12 T. R. Wang, P. Li and H. R. Li, *ACS Appl. Mater. Interfaces*, 2014, **6**, 12915-12921.
- 13 T. R. Wang, M. Q. Liu, Q. Ji and Y. G. Wang, *RSC Adv.*, 2015, **5**, 103433-103438.
- 14 B. D. Mather, K. Viswanathan, K. M. Miller and T. E. Long, *Prog. Polym. Sci.*, 2006, **31**, 487-531.
- 15 S. Kumari, B. Malvi, A. Kr. Ganai, V. K. Pillai and S. S. Gupta, *J. Phys. Chem. C*, 2011, **115**, 17774-17781.
- 16 Y. Kim, S. O. Ho, N. R. Gassman, Y. Korlann, E. V. Landorf, F. R. Collart and S. Weiss, *Bioconjugate Chem.*, 2008, **19**, 786-791.
- 17 W. W. Li, J. Heinze and W. Haehnel, *J. Am. Chem. Soc.*, 2005, **127**, 6140-6141.
- 18 M. Friedman, J. F. Cavins and J. S. Wall, *J. Am. Chem. Soc.*, 1965, **87**, 3672-3682.
- 19 Q. F. Li, Y. Yang, A. Maleckis, G. Otting and X. C. Su, *Chem. Commun.*, 2012, **48**, 2704-2706.
- 20 Q. F. Li, X. D. Du, L. Jin, M. M. Hou, Z. L. Wang and J. H. Hao, *J. Mater. Chem. C*, 2016, **4**, 3195-3201.
- 21 L. B. de. Paiva, A. R. Morales, F. R. V. Díaz, *Appl. Clay Sci.*, 2008, **42**, 8-24.
- 22 P. Podsiadlo, A. K. Kaushik, E. M. Arruda, A. M. Waas, B. S. Shim, J. D. Xu, H. Nandivada, B. G. Pumplun, J. Lahann, A. Ramamoorthy and N. A. Kotov, *Science*, 2007, **318**, 80-83.
- 23 J. E. Martin, A. J. Patil, M. F. Butler and S. Mann, *Adv. Funct. Mater.*, 2011, **21**, 674-681.
- 24 N. T. Whilton, S. L. Burkett, and S. Mann, *J. Mater. Chem.*, 1998, **8**, 1927-1932.
- 25 F. H. Ma, J. L. Chen, Q. F. Li, H. H. Zuo, F. Huang and X. C. Su, *Chem. Asian J.*, 2014, **9**, 1808-1816.
- 26 S. L. Burkett, A. Press and S. Mann, *Chem. Mater.*, 1997, **9**, 1071-1073.
- 27 D. M. Jenkins, *Phys. Chem. Minerals*, 1989, **16**, 408-414.
- 28 K. Liu, H. P. You, Y. H. Zheng, G. Jia, Y. H. Song, Y. J. Huang, M. Yang, J. J. Jia, N. Guo and H. J. Zhang, *J. Mater. Chem.*, 2010, **20**, 3272-3279.
- 29 H. Chen, Y. J. Xie, A. M. Kirillov, L. L. Liu, M. H. Yu, W. S. Liu and Y. Tang, *Chem. Commun.*, 2015, **51**, 5036-5039.
- 30 M. Ren, C. D. S. Brites, S. S. Bao, R. A. S. Ferreira, L. M. Zheng and L. D. Carlos, *J. Mater. Chem. C*, 2015, **3**, 8480-8484.
- 31 Z. Zhou and Q. M. Wang, *Nanoscale*, 2014, **6**, 4583-4587.
- 32 J. N. Hao and B. Yan, *Nanoscale*, 2016, **8**, 12047-12053.
- 33 Y. Zhou and B. Yan, *Chem. Commun.*, 2016, **52**, 2265-2268.
- 34 Y. J. Cui, W. F. Zou, R. J. Song, J. C. Yu, W. Q. Zhang, Y. Yang and G. D. Qian, *Chem. Commun.*, 2014, **50**, 719-721.
- 35 M. L. P. Reddy, V. Divya and R. Pavithran, *Dalton Trans.*, 2013, **42**, 15249-15262.
- 36 J. Liu, W. Zuo, W. Zhang, J. Liu, Z. Y. Wang, Z. Y. Yang and B. D. Wang, *Nanoscale*, 2014, **6**, 11473-11478.
- 37 A. L. Gassner, C. Duhot, J. C. G. Bünzli and A. S. Chauvin, *Inorg. Chem.*, 2008, **47**, 7802-7812.
- 38 J. B. Lamture, Z. H. Zhou, A. S. Kumar and T. G. Wensel, *Inorg. Chem.*, 1995, **34**, 864-869.
- 39 Q. F. Li, D. Yue, G. W. Ge, X. D. Du, Y. C. Gong, Z. L. Wang and J. H. Hao, *Dalton Trans.*, 2015, **44**, 16810-16817.
- 40 J. Feng and H. J. Zhang, *Chem. Soc. Rev.*, 2013, **42**, 387-410.
- 41 K. Binnemans, *Chem. Rev.*, 2009, **109**, 4283-4374.
- 42 Q. Wang, W. B. Wang and A. Q. Wang, *J. Control Release*, 2015, **213**, 91-92.
- 43 M. W. England, C. Urata, G. J. Dunderdale and A. Hozumi, *ACS Appl. Mater. Interfaces*, 2016, **8**, 4318-4322.
- 44 M. B. Gebeyehu, Y. H. Chang, A. K. Abay, S. Y. Chang, J. Y. Lee, C. M. Wu, T. C. Chiang and R. I. Murakami, *RSC Adv.*, 2016, **6**, 54162-54168.
- 45 M. Karbowski, J. Cichos and K. Buczek, *J. Phys. Chem. B*, 2014, **118**, 226-239.
- 46 Y. Z. Xu, J. G. Wu, W. X. Sun, D. L. Tao, L. M. Yang, Z. F. Song, S. F. Weng, Z. H. Xu, R. D. Soloway, D. F. Xu and G. X. Xu, *Chem. Eur. J.*, 2002, **8**, 5323-5331.
- 47 Y. Yao, Y. G. Wang, Z. Q. Li and H. R. Li, *Langmuir*, 2015, **31**, 12736-12741.
- 48 D. Q. Yang, Y. G. Wang, L. He and H. R. Li, *ACS Appl. Mater. Interfaces*, 2016, **8**, 19709-19715.
- 49 T. S. Chu, H. P. Liu, Y. Y. Yang, H. M. Wang, Y. S. Hu, Y. Wang, M. H. Yu and S. W. Ng, *J. Photochem. Photobiol. A: Chem.*, 2014, **294**, 38-43.
- 50 F. Zhang, Y. Wang, T. S. Chu, Z. H. Wang, W. Li and Y. Y. Wang, *Analyst*, 2016, **141**, 4502-4510.
- 51 G. X. Bai, M. K. Tsang and J. H. Hao, *Adv. Optical Mater.*, 2015, **3**, 431-462.
- 52 G. X. Bai, M. K. Tsang, H. J. Hao, *Adv. Funct. Mater.*, 2016, **26**, 6330-6350.